Effect of Sheet Distance on the Optical Properties of Vanadate Nanotubes

J. Cao,* J. Choi, and J. L. Musfeldt

Department of Chemistry, University of Tennessee, Knoxville, Tennessee 37996-1600

S. Lutta and M. S. Whittingham

Department of Chemistry and Institute for Materials Research, State University of New York, Binghamton, New York 13902-6000

Received November 4, 2003. Revised Manuscript Received December 10, 2003

We measured the optical properties of mixed-valent vanadium oxide nanotubes to investigate the charge degrees of freedom in these novel materials. The electronic structure strongly resembles that of other bulk, low-dimensional, and molecular vanadates. The 1.2-eV band is assigned as a superposition of V^{4+} d → d and $V^{4+} \rightarrow V^{5+}$ charge-transfer excitations, and the features above 3 eV are attributed to O 2p → V 3d charge-transfer excitations. The 5-eV excitation shows a modest sheet distance dependence, red-shifting with increasing sheet distance. We find that the optical gap is ∼0.56 eV at room temperature and ∼0.65 eV at 4.2 K. It does not depend systematically on tube size. At the same time, selected V−O−V stretching modes sharpen and red-shift with increasing sheet distance. We attribute these trends to the microscopic manifestations of strain, which changes with curvature. A low-frequency mode is observed at 113 cm^{-1}, which is assigned as the radial breathing mode of the VO_x nanotubes.

I. Introduction

Nanophase materials represent a field of fundamental interest because this unique class of compounds is connected with interesting solid-state physical and chemical properties that can be exploited for a variety of practical applications. The tubular structure provides a high aspect ratio, access to different contact regions, and the ability to assemble into more complex architectures. These characteristics make nanotubes very promising candidates for the realization of highly functional, effective, and resource-saving devices such as single-electron transistors, sensors, capacitors, and storage/release systems.[1−3] The discovery of carbon nanotubes revolutionized fundamental science at the nano scale.[4] More recently, the synthesis of inorganic fullerene-like materials such as MoS_2, WS_2, BN, TiO_2, $NiCl_2$, VO_x, and NbS_2 has attracted attention.[5−18] Among these interesting materials, the VO_x nanotubes are especially important because of their tunable physical and chemical properties.[18−23]

As a transition metal, vanadium displays a number of oxidation states and can thus form a wide variety of single- and mixed-valent compounds with different properties.[24] The VO_x ($x \sim 2.4$) tubes of interest here are mixed valent. They contain nearly equal numbers of V^{4+} and V^{5+} cations.[20−22] It is this mixed-valence character that seems to cause the VO_x sheet to "wrap". Thus, the VO_x nanotubes (VONT) are actually scrolls, consisting of vanadate layers between which organic molecules are intercalated.[19−23] The amine functions as a structure-directing agent. The distance between the layers of the scroll, typically called the "sheet distance", correlates linearly with the size of the template, provid-

* To whom correspondence should be addressed.

(1) Dai, H.; Hafner, J. H.; Rinzler, A. G.; Colbert, D. T.; Smalley, R. E. *Nature (London)* **1996**, *384*, 147.
(2) Tremel, W. *Angew. Chem., Int. Ed.* **1999**, *38*, 2175.
(3) Collins, P. G.; Bradley, K.; Ishigami, M.; Zettl, A. *Science* **2000**, *287*, 1801.
(4) Iijima, S. *Nature* **1991**, *354*, 56.
(5) Rao, C. N. R.; Nath, M. *Dalton Trans.* **2003**, 1.
(6) Remskar, M.; Mrzel, A.; Skraba, Z.; Jesih, A.; Ceh, M.; Demšar, J.; Stadelmann, P.; lévy, F.; Mihailovic, D. *Science* **2001**, *292*, 479.
(7) Tenne, R.; Margulis, L.; Genut, M.; Hodes, G. *Nature* **1992**, *360*, 444.
(8) Rosentsveig, R.; Margolin, A.; Feldman, Y.; Popovitz-Biro, R.; Tenne, R. *Chem. Mater.* **2002**, *14*, 471.
(9) Feldman, Y.; Wasserman, E.; Srolovitz, D. J.; Tenne, R. *Science* **1995**, *267*, 222.
(10) Lee, R. S.; Gavillet, J.; Lamy de la Chapelle, M.; Loiseau, A.; Cochon, J.-L.; Pigache, D.; Thibault, J.; Willaime, F. *Phys. Rev. B* **2001**, *64*, 121405.
(11) Chopra, N. G.; Luyken, R. J.; Cherrey, K.; Crespi, V. H.; Cohen, M. L.; Louie, S. G.; Zettl, A. *Science* **1995**, *269*, 966.
(12) Hoyer, P. *Langmuir* **1996**, *12*, 1411.
(13) Liu, S. M.; Gan, L. M.; Liu, L. H.; Zhang, W. D.; Zeng, H. C. *Chem. Mater.* **2002**, *14*, 1391.
(14) Hacohen, Y. R.; Grunbaum, E.; Tenne, R.; Sloan, J.; Hutchison, J. L. *Nature* **1998**, *395*, 336.
(15) Nath, M.; Rao, C. N. R. *J. Am. Chem. Soc.* **2001**, *123*, 4841.
(16) Shi, X.; Han, S.; Sanedrin, R. J.; Zhou, F.; Selke, M. *Chem. Mater.* **2002**, *14*, 1897.
(17) Hernandez, B. A.; Chang, K.-S.; Fisher, E. R.; Dorhout, P. K. *Chem. Mater.* **2002**, *14*, 480.
(18) Spahr, M. E.; Bitterli, P.; Nesper, R.; Müller, M.; Krumeich, F.; Nissen, H. U. *Angew. Chem., Int. Ed.* **1998**, *37*, 1263.
(19) Krumeich, F.; Muhr, H.-J.; Niederberger, M.; Bieri, F.; Schnyder, B.; Nesper, R. *J. Am. Chem. Soc.* **1999**, *121*, 8324.
(20) Muhr, H.-J.; Krumeich, F.; Schönholzer, U. P.; Bieri, F.; Niederberger, M.; Gauckler, L. J.; Nesper, R. *Adv. Mater.* **2000**, *12*, 231.
(21) Niederberger, M.; Muhr, H.-J.; Krumeich, F.; Bieri, F.; Günther, D.; Nesper, R. *Chem. Mater.* **2000**, *12*, 1995.
(22) Lutta, S.; Dobley, A.; Ngala, K.; Yang, S.; Zavalij, P. Y.; Whittingham, M. S. *Mater. Res. Soc. Symp.* **2002**, *703*, V8.3.
(23) Reinoso, J. M.; Muhr, H.-J.; Krumeich, F.; Bieri, F.; Nesper, R. *Helv. Chim. Acta* **2000**, *83*, 1724.
(24) Chirayil, T.; Zavalij, P. Y.; Whittingham, M. S. *Chem. Mater.* **1998**, *10*, 2629.

10.1021/cm035119w CCC: $27.50
Published on Web 01/21/2004

ing an opportunity to tune the size of the tubes.[20] At this time, the vanadium oxide layer is thought to be a double-sheet structure based on VO_6 octahedra and VO_4 tetrahedra, similar to that in BaV_7O_{16} and (en)-V_7O_{16}.[25,26] The VO_6 building-block units are so bent and elongated in the VONTs that they are effectively square pyramids. Indeed, structural renderings by Wörle et al.[26] emphasize the latter point by showing sheets of VO_5 square pyramids and VO_4 tetrahedra; the sixth oxygen atom, which would complete the octahedral coordination, is more than 2.4 Å away from the central V atom. Both corner- and edge-sharing arrangements appear in the structure.[25,26] The VONTs also display important electrochemical and optical limiting behavior, making them amenable to device applications.[27,28] Two such examples are battery materials (Mn^{2+} intercalated VONTs) and molecular electronics (VONTs coated carbon nanotubes).[29] It is notable that other inorganic nanotubes have also attracted attention because of their performance as SEM tip materials[30] and as a result of their unique mechanical properties.[31]

The electronic structure and vibrational properties of inorganic fullerene-like materials are of great current interest. Theoretical predictions of strain energy, optical gap, and electronic structure have focused on Si- and P-based tubes, NbS_2, MoS_2, WS_2, GaN, GaSe, and BN nanostructures.[32−40] In GaSe, GaN, and MoS_2, the energy gap is predicted to increase toward the bulk value as the tube diameter increases, whereas the strain energy decreases with increasing tube diameter.[35,37,38] In black phosphorus tubes, the gap also increases with chiral angle.[40] In BN nanotubes, vibrational property predictions suggest that the modes will red-shift with increasing tube diameter.[41] The frequency of the radial breathing mode is of special interest and is predicted to increase with decreasing tube diameter.[41] Broad and complementary spectroscopic measurements of inorganic fullerene-like materials have been more sparse. The optical properties of selected model materials (MoS_2, WS_2, and a selected VONT) have been studied over a limited energy range[28,42] In tubular MoS_2 and WS_2, the gap is lower than the corresponding bulk material, in line with the aforementioned theoretical predictions.[42] Photoluminescence emission of Y_2O_3:Eu nanotubes is also different from that in the bulk, displaying important surface structure and excitation wavelength effects.[43] Vibrational property measurements show broadened (MoS_2, WS_2, and HfS_2),[5] red-shifted (CdSe),[44] or identical ($NbSe_2$) phonon modes compared with analogous bulk materials.[5]

To investigate the charge degrees of freedom in vanadium oxide nanotubes and to understand the effect of sheet distance on the vibrational and electronic properties, we measured the optical absorption spectrum of a series of VONTs over a wide energy range. In these materials, the sheet distance is analogous to tube diameter (discussed above), as it controls the "winding" of the scroll. The sheet distance was adjusted with various amine templates, allowing us to alter the tube size. Thus, the effect of sheet distance on the optical properties could be examined. An additional motivation for this work is to provide an accurate picture of the electronic structure of VONTs, which can be used to understand the optical limiting mechanism in these materials.[28] Since the dynamics are very sensitive to local strain, we also seek to understand the effect of the sheet distance on the tube distortion by studying the vibrational properties of these materials.

II. Experimental Methods

A. Nanotube Synthesis and Sample Preparation. The vanadate nanotubes were prepared by an initial sol−gel reaction followed by hydrothermal treatment.[21,22] V_2O_5 and an appropriate amine template ($C_nH_{2n+1}NH_2$ with $n = 4-18$) were mixed in a 1:1 molar ratio in ethanol and stirred for 3 h in air. The mixture was then hydrolyzed under vigorous stirring followed by aging, which led to the formation of a yellow suspension. Subsequent hydrothermal treatment for 7 days resulted in a black powder. The product was washed with ethanol, diethyl ether, and water to remove excess amine and any decomposed products. The material was then dried under vacuum at 80 °C for 12 h. The nanotubes (henceforth abbreviated as C_n-VONT, where C_n refers to the number of carbon atoms in the structure-directing amine) were prepared with a variety of different amine templates, allowing control over the sheet distance. The tubular morphology of the product was confirmed by transmission electron microscopy, and the sheet distance was determined by X-ray diffraction. For our materials, the sheet distance varied between ∼15 and 35 Å.

The VONTs were mixed with pure KCl powder.[45] and pressed at 20000 psi to form isotropic pellets for transmission measurements. Different loading levels (∼0.05, 0.03, and 0.02 wt %) were employed as needed to obtain optimum sensitivity over the full energy range of our investigation. The VONTs were also pressed into pellets for reflectance measurements. In the latter, no matrix material was used.

B. Spectroscopic Measurements. Infrared transmittance and reflectance experiments were carried out over a wide energy range (from 4 meV to 7 eV; 30−56 000 cm^{-1}) using a series of spectrometers including a Bruker IFS 113V Fourier transform infrared spectrometer equipped with a bolometer

(25) Wang, X.; Liu, L.; Bontchev, R.; Jacobson, J. *Chem. Commun.* **1998**, 1009.
(26) Wörle, M.; Krumeich, F.; Bieri, F.; Muhr, H.-J.; Nesper, R. Z. *Anorg. Allg. Chem.* **2002**, *628*, 2778.
(27) Dobley, A.; Ngala, K.; Yang, S.; Zavalij, P. Y.; Whittingham, M. S. *Chem. Mater.* **2001**, *13*, 4382.
(28) Xu, J.-F.; Czerw, R.; Webster, S.; Carroll, D. L. Ballato, J.; Nesper, R.; *Appl. Phys. Lett.* **2002**, *81*, 1711.
(29) Ajayan, P. M.; Stephan, O.; Redlich, Ph.; Colliex, C. *Nature* **1995**, *375*, 564.
(30) Rothschild, A.; Cohen, S. R.; Tenne, R. *Appl. Phys. Lett.* **1999**, *75*, 4025.
(31) Zhu, Y. Q.; Sekine, T.; Brigatti, K. S.; Firth, S.; Tenne, R.; Rosentsveig, R.; Kroto, H. W.; Walton, D. R. M. *J. Am. Chem. Soc.* **2003**, *125*, 1329.
(32) Seifert, G.; Köhler, Th.; Urbassek, H. M.; Hernández, E.; Frauenheim, T. *Phys. Rev. B* **2001**, *63*, 193409.
(33) Seifert, G.; Hernández, E. *Chem. Phys. Lett.* **2000**, *318*, 355.
(34) Seifert, G.; Terrones, H.; Terrones, M.; Frauenheim, T. *Solid State Commun.* **2000**, *115*, 635.
(35) Seifert, G.; Terrones, H.; Terrones, M.; Jungnickel, G.; Frauenheim, T. *Phys. Rev. Lett.* **2000**, *85*, 146.
(36) Seifert, G.; Terrones, H.; Terrones, M.; Jungnickel, G.; Frauenheim, T. *Solid State Commun.* **2000**, *114*, 245.
(37) Lee, S. M.; Lee, Y. H.; Hwang, Y. G.; Elsner, J.; Porezag, D.; Frauenheim, T. *Phys. Rev. B* **1999**, *60*, 7788.
(38) Côté, M.; Cohen, M. L.; Chadi, D. J. *Phys. Rev. B* **1998**, *58*, R4277.
(39) Rubio, A.; Corkill, J. L.; Cohen, M. L. *Phys. Rev. B* **1994**, *49*, 5081.
(40) Cabria, I.; Mintmire, J. W. *Europhys. Lett.*, **2004**, *65*, 82−88.
(41) Sánchez-Portal, D.; Hernández, E. *Phys. Rev. B* **2002**, *66*, 235415.
(42) Frey, G. L.; Elani, S.; Homyonfer, M.; Feldman, Y.; Tenne, R. *Phys. Rev. B* **1998**, *57*, 6666.
(43) Wu, C.; Qin, W.; Qin, G.; Zhao, D.; Zhang, J.; Huang, S.; Lü, S.; Liu, H.; Lin, H. *Appl. Phys. Lett.* **2003**, *82*, 520.
(44) Teredesai, P. V.; Deepak, F. L.; Govindaraj, A.; Rao, C. N. R.; Sood, A. K. *J. Nanosci. Nanotechnol.* **2002**, *2*, 495.
(45) KCl is clear in the optical range.

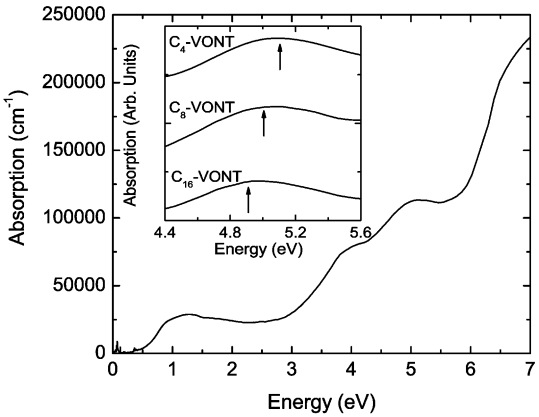

Figure 1. 300 K absorption spectrum of C_8-VONT. The inset shows a close-up view of one of the high-energy excitations, which changes modestly with sheet distance. In the inset, the curves are offset for clarity.

detector, a Bruker Equinox 55 Fourier transform infrared spectrometer equipped with a microscope attachment, and a modified Perkin-Elmer Lambda-900 grating spectrometer. A pure KCl pellet was employed as the reference during transmittance experiments, whereas an aluminum reference mirror was used during reflectance measurements. Our resolution was 2 cm^{-1} in the infrared and 2 nm in the optical regime.

Absorption was calculated from both transmission and reflectance measurements. This separate and independent determination of the lossy part of the optical response has several advantages, as discussed below. The absorption coefficient was obtained from the measured transmittance as $\alpha = (-1/hd)\ln T$, where h is the loading of C_n-VONT in the pellet and d is the pellet thickness.[46,47] The optical absorption coefficient was also calculated from the measured reflectance using a Kramers−Kronig analysis.[46,48] Here, α represents the lossy part of the dielectric response. Excellent agreement was obtained for the absorption, using the two different methods. Standard peak-fitting techniques were employed to assess sheet distance-dependent trends, as appropriate.[49]

Although the 300 K optical properties of the VONTs are likely to be of greatest interest to the battery and nonlinear optics community, we also performed variable temperature experiments to investigate the more fundamental aspects of the electronic structure of these materials. The search for size-dependent trends in the optical gap received particular attention. The low-temperature spectroscopies were carried out with a continuous-flow helium cryostat and temperature controller. Well-known effects of reduced temperature include line width reduction and the sharpening of the optical gap.[50−52]

III. Results and Discussion

A. Electronic Structure of the VONTs. Figure 1 displays the 300 K optical absorption spectrum of C_8-VONT, calculated from a Kramers−Kronig analysis of the reflectance spectrum.[46] The spectrum shows several reproducible, fairly prominent, broad bands, which are centered at ∼1.2, 3.9, 5.0, and 7.0 eV. The feature at ∼1.2 eV is assigned as the superposition of both V d → d and $V^{4+} \rightarrow V^{5+}$ charge-transfer excitations. The features centered at 3.9, 5.0, and ∼7.0 eV are assigned as O 2p → V 3d charge-transfer transitions. The inset shows a close-up view of the 5.0-eV excitation, which changes modestly with sheet distance.[53] This red-shift with increasing sheet distance is very unusual, different from traditional strain-induced red-shifting in other inorganic fullerene-like materials.[32−40] Unfortunately, the challenging crystal structure combined with the lack of theoretical work on the VONTs precludes a detailed explanation of this trend. We speculate that the 5-eV excitation is strongly polarized in the radial direction. This supposition can be checked, once oriented samples are available, and the result may connect it with the observed sheet distance effect. The optical gap, 2Δ, is determined by making a linear extrapolation of the leading edge of the absorption band down to zero energy. For C_8-VONT, we find $2\Delta_{300K} \sim 0.54$ eV. At low temperature, the gap sharpens and moves to higher energy. The shape of the optical gap is similar to that of other synthetic metal materials.[54−57]

Table 1. Optical Gap of Different VONTs

material	sheet distance (Å)	$2\Delta_{300K}$[a] (eV)	$2\Delta_{4.2K}$[a] (eV)
C_4-VONT	15.82	0.58	0.64
C_6-VONT	17.37	0.59	0.70
C_8-VONT	22.98	0.54	0.58
C_{12}-VONT	27.25	0.57	0.63
C_{14}-VONT	29.54	0.58	0.68
C_{16}-VONT	31.38	0.56	0.70
C_{18}-VONT	35.28	0.54	0.64
average value		0.56	0.65

[a] The error bar on 2Δ is 5% at 300 K and 3% at 4.2 K.

The sheet distance dependence of the optical gap is important for understanding the electronic structure of the VONTs. For several model materials, 2Δ is predicted to decrease from the bulk value with decreasing tube diameter.[35,37,38,40] This trend can be understood as the strain dependence of the electronic states in these compounds.[5] However, in our materials, changes in the sheet distance, analogous to the aforementioned tube diameter modifications, have no systematic effect on the optical gap (Table 1). On average, the gap, 2Δ, is ∼0.56 eV at 300 K and ∼0.65 eV at 4.2 K. We suspect that the insensitivity of the optical gap to sheet distance is related to the large diameter (∼100 nm) of the VONTs.[58] Upon substitution of different amine templates, there is only modest change in curvature. Thus, the potential effect of microscopic strain is minimized in the VONTs.

Comparing the absorption spectrum of C_8-VONT to that of other vanadates, we find that the VONTs show a striking resemblance to several model materials, including VO_2, α'-NaV_2O_5, and $Na_2V_3O_7$ (Figure 2),[59−63]

(46) Wooten, F. *Optical Properties of Solids*; Academic Press: New York, 1972.
(47) The typical error bars on an absolute level of absorption are about 10−15%.
(48) The high-energy reflectance was extrapolated as ω^{-1}, and the low-energy reflectance was extrapolated as a constant, appropriate for a semiconductor.
(49) We used Voight oscillators in the fitting precedure.
(50) Abay, B.; Güder, H. s.; Efeoğlu, H.; Yoğurtçu, Y. K. *J. Phys. Chem. Solids* **2001**, *62*, 747.
(51) Surendran, S.; Pokornỳ, J.; Jurek, K.; Bernstein, E.; Maly, P. *Mater. Sci. Eng. B* **2003**, *104*, 54.
(52) Shirakata, S.; Kondow, M.; Kitatani, T. *J. Phys. Chem. Solids* **2003**, *64*, 1533.
(53) To find the precise peak position of these bands, we set the derivative of the curve equal to zero.
(54) McKenzie, R. H.; Wilkins, J. W. *Phys. Rev. Lett.* **1992**, *69*, 1085.
(55) Long, F. H.; Love, S. P.; Swanson, B. I.; McKenzie, R. H. *Phys. Rev. Lett.* **1993**, *71*, 762.
(56) Kim, K.; McKenzie, R. H.; Wilkins, J. W. *Phys. Rev. Lett.* **1993**, *71*, 4015.
(57) Rudko, G. Yu.; Long, V. C.; Musfeldt, J. L.; Koo, H.-J.; Whangbo, M.-H.; Revcolevschi, A.; Dhalenne, G.; Bernholdt, D. E. *Chem. Mater.* **2001**, *13*, 939.
(58) Note that the tube diameters of GaSe and GaN, for instance, are smaller than those of the VONTs, and tube curvature is much more substantial.[37,38]

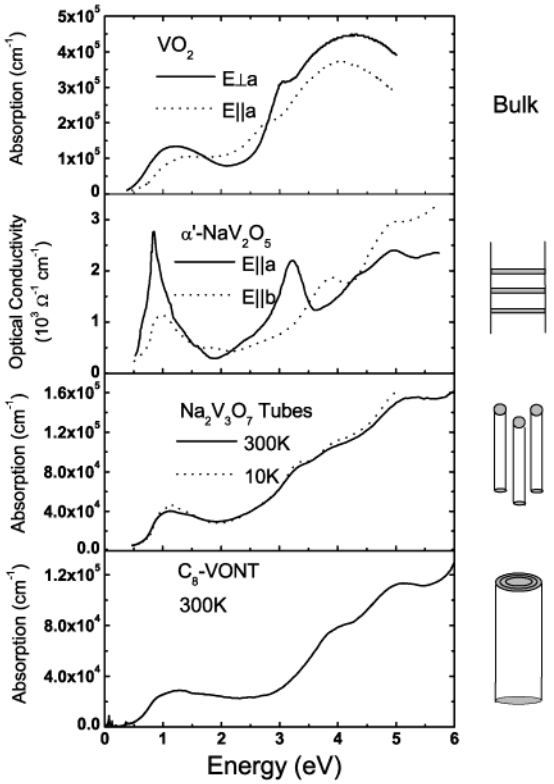

Figure 2. 300 K optical absorption spectrum of C_8-VONT as compared with the room-temperature absorption spectra of VO_2,[61] the polarized optical conductivity of α'-NaV_2O_5[59,62] and the variable temperature absorption spectra of $Na_2V_3O_7$.[63]

despite substantial differences in structure and charge. The absorption spectrum also resembles that of the molecule-based magnet $K_6[V_{15}As_6O_{42}(H_2O)]\cdot 8H_2O$.[64] In bulk VO_2, tubular $Na_2V_3O_7$, and molecular $K_6[V_{15}As_6O_{42}(H_2O)]\cdot 8H_2O$, all transition metal atoms have a +4 charge. In these materials, the feature centered at ~1.2 has been assigned as a localized d → d transition between ground and excited states, split by a crystal field.[62−64] Assignment of the 1-eV excitation and the higher energy sidebands in ladder-like α'-NaV_2O_5, however, has been controversial due to the mixed-valence character of this material.[59,60,65] The 1-eV excitation is currently attributed to $V^{4+} \rightarrow V^{5+}$ charge-transfer excitations on the V−O−V rung.[60,65]

The VONTs are also mixed-valent, suggesting that the feature at ~1.2 eV may share certain characteristics with α'-NaV_2O_5. In our case, however, the band seems to arise from two sources, and we attribute it to the superposition of both V d → d and $V^{4+} \rightarrow V^{5+}$ charge-transfer excitations. Evidence for this dual assignment comes from both spectral and structural data. From the spectral point of view, both the band shape as well as the trend with decreasing temperature point toward contributions from two very different excitations in C_8-VONT. At 300 K, the band consists of two peaks: a weak feature at ~0.8 eV and a stronger feature centered at 1.2 eV. The 0.8 eV feature blue-shifts with decreasing temperature and combines with the 1.2-eV band at base temperatures. It is useful to recall that charge-transfer transitions often exhibit substantial temperature dependence, whereas on-site d → d excitations show more subtle effects. This difference suggests that the feature centered at 0.8 eV can be attributed to a $V^{4+} \rightarrow V^{5+}$ charge-transfer excitation and the larger 1.2-eV feature assigned as a V d → d excitation. Note that the d → d excitation is formally La Porte forbidden. It appears in the spectrum of the VONTs due to symmetry breaking around the chromophore, which relaxes the selection rules on excitations within the d manifold.[66] This kind of selection rule relaxation appears in a number of model vanadates.[61−64] Structural data also support the dual assignment of the ~1.2-eV band. As discussed previously, the mixed-valent chromophore units display both edge- and corner-sharing arrangements.[25,26] Only the edge-sharing units are likely to engage in charge transfer with appreciable oscillator strength; corner-sharing will likely not provide sufficient overlap for related excitations to appear in the spectrum. Combined with the La Porte forbidden on-site V d → d excitations, we can therefore account for the two oscillators that constitute the ~1.2-eV band.

The higher energy spectral features of the VONTs also display strong similarities with the aforementioned model vanadates, but the response is not identical (Figure 2). The structures at 3.9, 5.0, and ~7.0 eV, previously identified as O 2p → V 3d charge-transfer excitations in the VONTs, are present in the spectra of the bulk, ladder, and molecular materials.[59−64] However, the ~3.2-eV excitation that appears in the response of all other vanadates is not apparent in the spectrum of C_8-VONT (Figure 2) or the other VONTs. Future electronic structure calculations may be able to explain the absence of this feature in the VONTs.

Armed with an understanding of the electronic properties of the VONTs, we are now in a better position to shead light on the mechanism of optical limiting behavior in these materials.[28] Briefly, the findings of Xu et al. are that optical limiting is observed when the system is pumped at 532 nm (2.3 eV) but not when the system is pumped at 1064 nm (1.16 eV).[28] This is obviously different from the broadband nature of the limiting effect in carbon.[67,68] On the basis of these observations and the assignment of a 460-nm (2.7 eV) optical gap, the authors attribute the optical limiting effect to a two-photon process.[28] In this work we show, however, that the average optical gap of the VONTs is ~0.56 eV at 300 K, much less than that assumed by Xu et. al. The proposed two-photon mechanism[28] is therefore not consistent with this new picture of the electronic

(59) Long, V. C.; Zhu, Z.; Musfeldt, J. L.; Wei, X.; Koo, H.-J.; Whangbo, M.-H.; Jegoudez, J.; Revcolevschi, A. *Phys. Rev. B* **1999**, *60*, 15721.
(60) Presura, C.; Van der Marel, D.; Dischner, M.; Geibel, C.; Kremer, R. K. *Phys. Rev. B* **2000**, *62*, 16522.
(61) Verleur, H. W.; Barker, A. S., Jr.; Berglund, C. N. *Phys. Rev.* **1968**, *172*, 788.
(62) Shin, S.; Suga, S.; Taniguchi, M.; Fujisawa, M.; Kanzaki, H.; Fujimori, A.; Daimon, H.; Ueda, Y.; Kosuge, K.; Kachi, S. *Phys. Rev. B* **1990**, *41*, 4993.
(63) Choi, J.; Musfeldt, J. L.; Wang, Y. J.; Koo, H.-J.; Whangbo, M.-H.; Galy, J.; Millet, P. *Chem. Mater.* **2002**, *14*, 924.
(64) Choi, J.; Sanderson, L. A. W.; Musfeldt, J. L.; Ellern, A.; Kögerler, P. *Phys. Rev. B* **2003**, *68*, 064412.
(65) Sushkov, A. B.; Musfeldt, J. L.; Wei, X.; Crooker, S. A.; Jegoudez, J.; Revcolevschi, A. *Phys. Rev. B* **2002**, *66*, 054439.
(66) On-site V 3d−3d excitation is usually not allowed due to symmetry selection rules.
(67) Chen, P.; Wu, X.; Sun, X.; Lin, J.; Ji, W.; Tan, K. L. *Phys. Rev. Lett.* **1999**, *82*, 2548.
(68) Riggs, J. E.; Walker, D. B.; Carroll, D. L.; Sun, Y.-P. *J. Phys. Chem. B* **2000**, *104*, 7071.

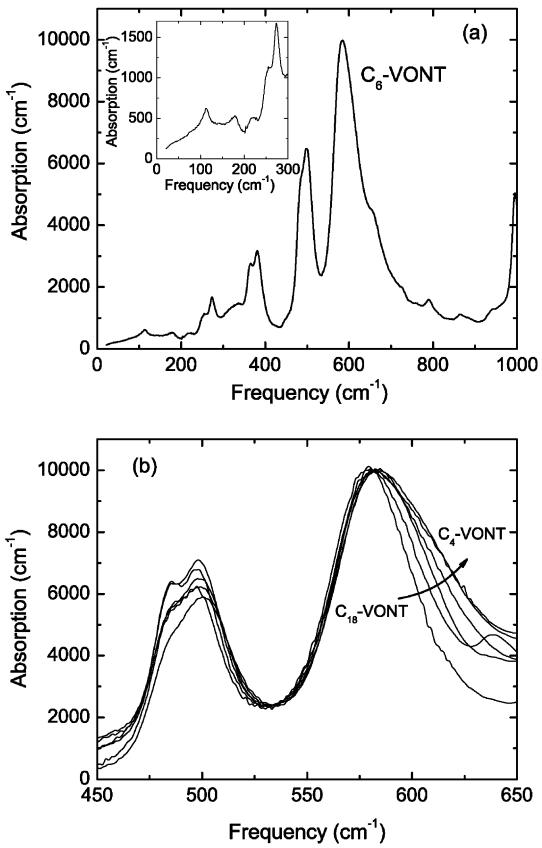

Figure 3. (a) 300 K infrared absorption spectrum of C_6-VONT. The inset shows a magnified view of the far-infrared response. (b) Close-up view of two V−O−V stretching modes as a function of sheet distance in the nanotubes.

structure, suggesting that it may be useful to consider alternate mechanisms for the optical limiting behavior in these materials. It is also useful to note that even if we assume that the band structure and gap assignment of the previous authors is correct, alternate explanations may be applied to their results. For instance, 532-nm excitation may promote a carrier into a virtual or "trapped" state, close to the conduction band, so that subsequent thermal excitation can take place. Low-temperature measurements could rule out this possibility. Pumping at a different energy, where thermal processes are unlikely (for instance, 1.9 eV), may also help to test the plausibility of this mechanism. Finally, we note that 1064-nm (1.16 eV) light will be absorbed into the band centered at ∼1.2 eV (Figure 1). For some reason, this seems to be an inappropriate choice from the point of view of optical limiting, perhaps forcing the system into a "wrong" excited state. On the other hand, 532-nm (2.3 eV) pumping successfully generates an optical limiting response in the VONTs, a result that may be related to the relatively low absorption window of the VONTs in this energy range. Electronic structure calculations, once available, may offer additional mechanistic insight.

B. Vibrational Structure of the VONTs. Figure 3a displays the 300 K vibrational response of C_6-VONT. The far- and middle-infrared absorption spectra display a number of modes that can be conveniently divided into four groups. These features are located at ∼113 cm^{-1}, between 150 and 400 cm^{-1}, between 400 and 1000 cm^{-1}, and above 1000 cm^{-1}. The modes above 1000 cm^{-1} are attributed to those of the amine template. Using previous mode assignments of other model vanadates including V_2O_5, α′-NaV_2O_5, $Na_2V_3O_7$, and $K_6[V_{15}As_6O_{42}(H_2O)]\cdot 8H_2O$ as well as the current understanding of the VONT structure,[25,26] the clusters located between 150 and 400 cm^{-1} and 400−1000 cm^{-1} are attributed to V−O bending and stretching, respectively.[64,65,69] There are two distinct axial stretching modes, a consequence of the substantial difference in the two axial V−O bond lengths, one of which is extremely long and weak. As expected, the axial modes are relatively insensitive to tube diameter effects. Selected equatorial stretching modes do, however, depend on the sheet distance, as detailed below. The isolated feature at 113 cm^{-1} (inset of Figure 3a) is assigned as the radial breathing mode of the tube and is also discussed in detail below. Our mode assignments are summarized in Table 2.

Table 2. Vibrational Modes of C_6-VONT[a]

peak frequency (cm^{-1})	assignment
113	radial breathing mode
179	V−O bending
215	V−O bending
255, 273[b]	V−O bending
341, 366, 381[b]	V−O bending
486, 498[b]	V−O−V (weak axial) stretching[c]
585[b],653,727	V−O−V (equatorial) stretching
790	V−O−V (equatorial) stretching
866	V−O−V (equatorial) stretching
945, 995[b]	V−O (strong axial) stretching[d]

[a] The features above 1000 cm^{-1} are related to the motion of the amine template. [b] Indicates the main feature in a multipeak cluster. [c] Oxygen is shared by two vanadiums. [d] Oxygen is not shared by two vanadiums.

We find that selected vanadium−oxygen stretching modes are very sensitive to tube curvature. Figure 3b shows a close-up view of two V−O−V stretching modes as a function of sheet distance.[70] The peak centered at ∼585 cm^{-1} appears to broaden with decreasing sheet distance. This widening is somewhat of an optical illusion, as discussed below. More modest sheet distance effects are observed in the ∼490-cm^{-1} feature. To quantify the changes in the vibrational properties with sheet distance, we fit the various spectra with five model oscillators over the frequency range of interest, 450−700 cm^{-1}. Figure 4a gives an example of a typical fit.[71]

The peak positions and integrated areas of the four most important oscillators are shown in Figure 4b,c as a function of sheet distance. The trends associated with the ∼585-cm^{-1} feature are notable. The center peak positions of oscillators 3 and 4 converge by ∼12 cm^{-1} over the range of our investigation (C_4-VONT to C_{18}-VONT), whereas the center positions of oscillators 1 and 2 display a more modest frequency change, converging by only ∼2 cm^{-1}. The integrated areas of oscillators 3 and 4 increase and decrease with increasing sheet distance, respectively, indicating a transfer of spectral weight from the high-energy sideband (oscillator 4) to the main peak (oscillator 3). This trend is consistent with more pronounced (limited) site distinction on smaller (larger) tubes. In contrast, the integrated areas

(69) Popova, M. N.; Sushkov, A. B.; Golubchik, S. A.; Mavrin, B. N.; Denisov, V. N.; Malkin, B. Z.; Iskhakova, A. L.; Isobe, M.; Ueda, Y. *J. Exp. Theor. Phys.* **1999**, *88*, 1186.

(70) The spectra have been normalized so that it is meaningful to compare the integrated area.

(71) The fifth oscillator works as a background.

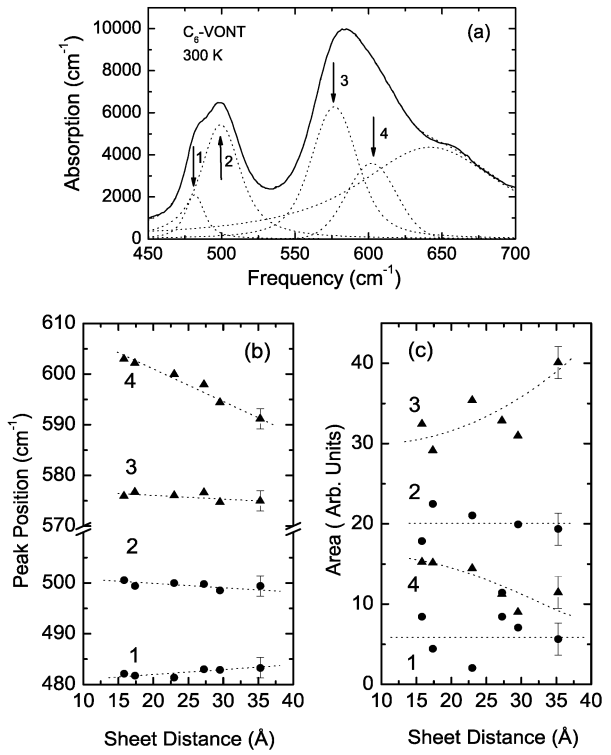

Figure 4. (a) Example fit of the 300 K spectrum of C_6-VONT in the range of the V−O−V stretching modes. Dashed lines show the model Voight oscillators used in the fit. (b) Peak positions of the fitted oscillators as a function of sheet distance. (c) Integral areas of the fitted oscillators vs sheet distance. Dashed lines guide the eye.

of oscillators 1 and 2 (associated with the ∼490-cm^{-1} feature) are insensitive to sheet distance effects.

We attribute these trends to tube curvature effects. From the structural point of view, tube curvature increases as sheet distance decreases (from C_{18}-VONT to C_4-VONT). When a two-dimensional sheet is wrapped into the tubular morphology, equatorial bond lengths and their motion will be especially sensitive to the degree of radial distortion. Greater distortion will manifest itself in the spectrum in several ways, typically with mode shifting, line width changes, and site-symmetry breaking. All are observed in the VONTs (Figure 3b). The sensitivity of the 580-cm^{-1} feature to sheet distance modification is therefore directly attributable to the directional character of the V−O−V equatorial stretching motion and the distortion of the nanotube. The overall red-shifting with increasing sheet distance, characteristic of a more relaxed lattice, is especially pronounced. In contrast, axial bond lengths (and their associated vibrational motion) are modified only subtly due to distortion. Sheet distance effects on the ∼490-cm^{-1} mode (related to the very long V−O−V axial stretching motion in the sheet) are in line with this supposition.

Previous far-infrared studies of other model vanadates indicate that the lowest frequency modes are not due to localized vibrations of vanadium and oxygen atoms, but instead are related to more complicated, long-range external motions such as lattice motion, liberation, or rattling.[69,72] For instance, the 74-cm^{-1} feature in V_2O_5 is assigned as a librational mode of the $(V_2O_5)_n$ chains,[72] the 90-cm^{-1} mode in α′-NaV_2O_5 is attributed to translation of V_2O_5 units along the *c* axis,[69] the 88-cm^{-1} mode in $Na_2V_3O_7$ is connected with the rattling mode of Na^+ inside the tubes,[63] and the 85-cm^{-1} feature in $K_6[V_{15}As_6O_{42}(H_2O)]\cdot 8H_2O$ is assigned as a rattling mode of H_2O inside the vanadium oxide cage.[64] None of these options offer a plausible assignment for the 113-cm^{-1} feature in the VONTs. However, the morphology of the VONTs suggests an interesting alternative. Theoretical and experimental work indicate that, in the tubular morphology, a low-frequency radial breathing mode is expected. For instance, in single-wall carbon nanotubes and BN tubes, the frequency of the radial breathing mode is inversely proportional to the radius of the nanotube, independently of the nanotube structure.[73,41] For the BN tubes, this red-shifting is predicted to be substantial, moving from 600 to 100 cm^{-1} as the tube radius increases from 2.5 to 10 Å.[41] A peak at 113 cm^{-1} is therefore the correct order of magnitude for assignment as a radial breathing mode in the VONTs. Considering the theoretical predictions, it is somewhat disappointing to find that the 113-cm^{-1} feature does not display any sheet distance dependence. We attribute this lack of sensitivity to the small difference of sheet distances compared with large tube diameters.

Conclusion

We report the optical properties of a series of mixed-valent vanadium oxide nanotubes over a wide energy range. The sheet distance was adjusted with various amine templates, allowing us to alter the tube size. Thus, the effect of sheet distance on the optical properties could be examined. The electronic structure of the VONTs strongly resembles that of other bulk, low-dimensional, and molecular vanadates. The 1.2-eV band is assigned as a superposition of V^{4+} d → d and $V^{4+} \rightarrow V^{5+}$ charge-transfer excitations, and the features above 3 eV are attributed to O 2p → V 3d charge-transfer excitations. Evidence for the dual character of the 1.2-eV band comes from both spectral and structural data, in particular, the band shape as well as trends with decreasing temperature. The 5-eV excitation shows a modest sheet distance dependence, red-shifting with increasing tube diameter. We find that the optical gap is ∼0.56 eV at room temperature and ∼0.65 eV at 4.2 K. Although it varies with temperature, the optical gap does not depend systematically on tube size. At the same time, selected V−O−V stretching modes sharpen and red-shift with increasing sheet distance. We attribute these trends to the microscopic manifestations of strain, which changes with curvature. A low-frequency mode is observed at 113 cm^{-1}, which is assigned as the radial breathing mode of the VO_x nanotubes.

Acknowledgment. Work at the University of Tennessee is supported by the Materials Science Division, Office of Basic Energy Sciences at the U.S. Department of Energy under Grant DE-FG02-01ER45885. The work at Binghamton is supported by the National Science Foundation through Grant DMR0313963. We thank M.-H. Whangbo for useful conversations.

CM035119W

(72) Abello, L.; Husson, E.; Repelin, Y.; Lucazeau, G. *Spectrochim. Acta* **1983**, *39A*, 641.
(73) Kürti, J.; Kresse, G.; Kuzmany, H. *Phys. Rev. B* **1998**, *58*, R8869.